electron-phonon collisions is smaller than 1.4×10^{-4} cm. As would be expected, the zero-temperature energy gap of the bulk material is not affected by an external magnetic field which is much smaller than the critical field.

ACKNOWLEDGMENTS

The authors would like to thank Reynold Kagiwada for his help in the performance of these experiments, and J. L. Brewster for designing and building most of the equipment.

PHYSICAL REVIEW VOLUME 132, NUMBER 3 1 NOVEMBER 1963

Deformation Potentials in Silicon. III. Effects of a General Strain on Conduction and Valence Levels*

IZA GOROFF† AND LEONARD KLEINMAN
Department of Physics and Laboratory for Research on the Structure of Matter, University of Pennsylvania, Philadelphia, Pennsylvania
(Received 25 June 1963)

Using a self-consistent perturbation theory developed in the first two papers of this series we have calculated the deformation potentials for a general strain for points of high symmetry (Γ, X, and L) in the conduction and valence bands of Si. We compare our calculated results with experimental values for (1) hydrostatic-pressure dependence of various energy gaps, (2) uniaxial-strain dependence of the splitting of the fourfold degenerate level at the top of the valence band, and (3) uniaxial strain dependence of the splitting of the degeneracy between equivalent valleys at the bottom of the conduction band. The agreement between theory and experiment ranges from fair to good.

I. INTRODUCTION

THE change in energy caused by an arbitrary strain is calculated here for states of high symmetry near the top of the valence band and the bottom of the conduction band in Si. The experimental studies of these effects can be grouped into three classes. (1) The fourfold degenerate $\Gamma_{25'}$ ($j=\frac{3}{2}$) level at the top of the valence band is split into two twofold levels by a general uniaxial strain. Hensel and Feher[1] have measured the cyclotron-resonance-effective masses of holes at the top of the valence band in Si as a function of strain and, thus, were able to calculate the strain-induced splitting of these levels. In the first paper of this series[2] (hereafter called I) the theory of the strain splitting of the top of the valence band is presented, and three other experiments performed on the holes to measure this splitting are briefly discussed. (2) Donor impurity electron wave functions in Si consist of linear combinations of conduction electron wave functions in the six valleys along the equivalent [100] directions in k space. Because of central cell corrections to the effective mass formalism[3] (chemical shifts), that combination of conduction-electron wave functions which adds in phase at the impurity site lies lowest in energy. When a uniaxial strain is applied along one of the valley directions, the intervalley degeneracy is destroyed and the lower lying valleys contribute a greater proportion to the impurity wave function. Thus, by measuring the amplitude of the wave function at the impurity site as a function of strain, Wilson and Feher[4] (by means of the hyperfine splitting of electron-spin-resonance lines in strained Si) measured the intervalley splitting. Similarly, a measurement of the strain dependence of the ionization energy of the donor electrons[5] leads to the intervalley strain splitting. (3) Paul and co-workers[6–8] have measured the shifts in the optical absorption peaks and, hence, in their associated energy gaps as a function of hydrostatic pressure. Unfortunately, most of the data is for Ge but the *pressure* dependence of any particular gap seems to be fairly constant among all the diamond and zinc-blende semiconductors.[9] Paul *et al.* have measured the pressure dependence of the indirect ($\Gamma_{25'}-\Delta_1$) gap in Si both by conductivity measurements and by direct observation of the shift of the indirect-transition edge. Philipp, Dash, and Ehrenreich[10] have attempted to map the motion of the band structure of Si under a bending type of strain which had both a hydrostatic and a uniaxial (either [100] or [111]) component. In view of the complexity of the behavior of the band structure under such a strain (see Sec. II) and the breadth of the re-

* Supported by the Advanced Research Projects Agency.
† National Science Foundation Cooperative Predoctoral Fellow during the time of this research.
[1] J. C. Hensel and G. Feher, Phys. Rev. **129**, 1041 (1963).
[2] L. Kleinman, Phys. Rev. **128**, 2614 (1962).
[3] W. Kohn, in *Solid State Physics*, edited by F. Seitz and D. Turnbull (Academic Press Inc., New York, 1957), Vol. 5, p. 258.
[4] D. K. Wilson and G. Feher, Phys. Rev. **124**, 1068 (1961).
[5] H. Fritzsche, Phys. Rev. **115**, 336 (1959).
[6] W. Paul, J. Phys. Chem. Solids **8**, 196 (1959).
[7] W. Paul and D. M. Warschauer, J. Phys. Chem. Solids **5**, 89 and 102 (1958).
[8] M. Cardona and W. Paul. J. Phys. Chem. Solids **17**, 138 (1960).
[9] W. Paul. J. Appl. Phys. **32**, 2082 (1961).
[10] H. R. Philipp, W. Dash, and E. Ehrenreich, Phys. Rev. **127**, 762, (1962).

flection peaks, it is not too surprising that they were unsuccessful.

The absolute shift of the bottom of the conduction band or top of the valence band under hydrostatic pressure cannot be measured directly. These are of interest because each represents one of the components of the electron-phonon or hole-phonon coupling tensor. Herring *et al.*[11] have used this fact to obtain an experimental value for the conduction band shift. Unfortunately, the relaxation times required for Herring's theory vary markedly depending on whether they are obtained from transport measurements or cyclotron resonance.[12] (See the second paper in this series,[13] hereafter called II.)

In the next section we give a brief introduction to the techniques of the calculation (which are discussed thoroughly in I and II) and give a rather complete description of the response of the Γ, X, and L energy levels to a general strain. In the last section we compare the results of this calculation with all the available experimental data.

II. CALCULATIONS

We write the Hamiltonian for the electrons in the unstrained crystal as a sum of three terms.

$$\mathcal{H}=\mathcal{H}_{KE}+\mathcal{H}_{PE}+\mathcal{H}_R, \tag{1}$$

where the $\mathcal{H}_R$ is a nonlocal potential corresponding strictly to the orthogonalization terms in an orthogonalized plane wave[14] calculation. In I we showed that the perturbation Hamiltonian due to a dilationless uniaxial strain is a sum of five terms.

$$\mathcal{H}'=\mathcal{H}_{KE}'+\mathcal{H}_{PE}'+\mathcal{H}_R'+\zeta\mathcal{H}_{PE}{}^{B'}+\zeta\mathcal{H}_R{}^{B'}. \tag{2}$$

The first three terms would be all of the perturbation if the structure factor remained unchanged under the strain. Under a uniaxial strain along one of the [100] directions the structure factor remains unchanged and the "bond bending" terms are zero. But if the uniaxial strain is applied in a [111] or [110] direction, inner displacements may occur and the relative position of the two atoms in the unit cell is not uniquely determined. The case where the atoms move to keep all nearest-neighbor bond lengths unchanged corresponds to $\zeta=1$. $\zeta=0$ corresponds to intracellular distances transforming according to the macroscopic strain tensor and the structure factor remaining unchanged. In I, we claimed that $\zeta=1$ was required to obtain the experimental[1] ratio of [100] and [111] $\Gamma_{25'}$ deformation potential constants. The present computer calculation has unearthed several errors in the original hand calculation and the value required to fit the experimental ratio is $\zeta=0.81$.

Following a suggestion in I, Segmuller[15] has measured ζ for Ge using x-ray diffraction; he finds $\zeta=0.7$. A first-principles calculation of ζ is underway[16] but since, like the elastic constants, it is second order in the strain, the accuracy of the calculation should not be expected to be as good as the accuracy of the present deformation potential calculation. In order to show the sensitivity of the various levels to inner displacements, we give the deformation potentials for both $\zeta=0.7$ and $\zeta=0.81$.

In II, we wrote the Hamiltonian for a unit hydrostatic strain perturbation

$$\mathcal{H}'=\mathcal{H}_{KE}'+\mathcal{H}_{PE}'+\mathcal{H}_R'+\delta V_{000}, \tag{3}$$

where V_{000} consists of core-valence exchange, valence-valence exchange, and valence-valence correlation terms as well as a large many-electron, many-ion Coulomb term. All these terms except for the valence-valence exchange are either independent of energy level or are very small so that they are of no interest when discussing relative shifts between energy levels. In II, the valence-valence exchange term was calculated for $\Gamma_{25'}$, the top of the valence band, by assuming it to be the same as the exchange energy of a free electron at the top of the Fermi sea. Phillips and Kleinman[17] have calculated matrix elements of the screened Hartree-Fock exchange operator from which the screened energy of the states $\Gamma_{25'}$, Γ_{15}, and $X_1{}^{(2)}$ may be estimated (in their approximation only the screened part of the exchange energy varied from state to state). One finds the screened exchange energy of $X_1{}^{(2)}$ and Γ_{15} to be 20 and 32% less than that of $\Gamma_{25'}$ ($E_{\text{screened ex}}{}^{\Gamma_{25'}}=-0.326$ Ry). However, $E_{\text{ex}}{}^{\Gamma_{25'}}=-1.221r_s{}^{-1}=-0.61$ Ry, so that the total exchange energy of $X_1{}^{(2)}$ and Γ_{15} is only about 11 and 17% less than that of $\Gamma_{25'}$. This drop in exchange energy for states just above the energy gap corresponds to the infinity in dE^{ex}/dk at $k=K_F$ in a free-electron gas. Because the percentages just quoted are only approximate, we take the valence-valence exchange contribu-

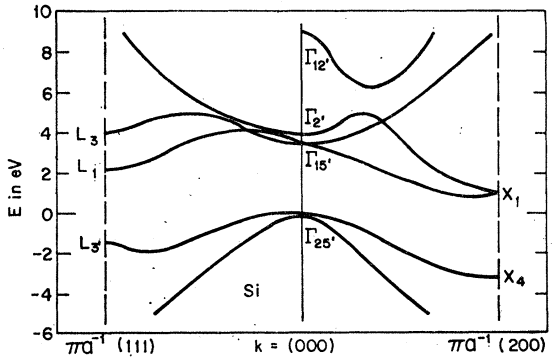

FIG. 1. The Si band structure taken from J. C. Phillips, Phys. Rev. **125**, 1931 (1962).

[11] C. Herring and E. Vogt, Phys. Rev. **101**, 944 (1956); and C. Herring, T. H. Geballe, and J. E. Kunzler, Bell System Tech. J. **38**, 657 (1959).
[12] D. M. S. Bagguley, D. W. Flaxen, and R. A. Stradling, Phys. Letters **1**, 111 (1962).
[13] L. Kleinman, Phys. Rev. **130**, 2283 (1963).
[14] C. Herring, Phys. Rev. **57**, 1169 (1940).
[15] A. Segmuller, Phys. Letters **4**, 227 (1963).
[16] I. Goroff and L. Kleinman (to be published).
[17] J. C. Phillips and L. Kleinman, Phys. Rev. **128**, 2098 (1962).

TABLE I. Listed is the calculated change in energy (in eV/ε) of each level under the indicated strains. The levels, whose deformation potential constants are preceded by a ±, are split under the indicated strain. The L_3 and $L_{3'}$ levels are split by spin-orbit coupling in addition to the strain splitting. The linear relation given above for the L_3 and $L_{3'}$ splitting hold only when $\Delta_{\text{strain}} \gg \Delta_{so}$. [See Eq. (5).]

Level \ Strain tensor	$\varepsilon\begin{pmatrix}1&0&0\\0&1&0\\0&0&1\end{pmatrix}$	$2\varepsilon\begin{pmatrix}1&0&0\\0&-\frac{1}{2}&0\\0&0&-\frac{1}{2}\end{pmatrix}$	$\xi=0.81$ $\varepsilon\begin{pmatrix}0&1&1\\1&0&1\\1&1&0\end{pmatrix}$	$\zeta=0.7$ $\varepsilon\begin{pmatrix}0&1&1\\1&0&1\\1&1&0\end{pmatrix}$	$\zeta=0.81$ $\varepsilon\begin{pmatrix}0&0&0\\0&0&1\\0&1&0\end{pmatrix}$	$\zeta=0.7$ $\varepsilon\begin{pmatrix}0&0&0\\0&0&1\\0&1&0\end{pmatrix}$
$\Gamma_{2'}$	−10.7	0	0	0	0	0
Γ_{15} $(j=\frac{1}{2})$	−3.44	0	0	0	0	0
Γ_{15} $(j=\frac{3}{2})$	−3.44	±1.10	±2.92	±3.18	±2.92	±3.18
$\Gamma_{25'}$ $(j=\frac{1}{2})$	−2.09	0	0	0	0	0
$\Gamma_{25'}$ $(j=\frac{3}{2})$	−2.09	±2.49	±3.28	±2.79	±3.28	±2.79
$L_1^{(2)}$ ([111])	−6.20	0	11.4	11.5	11.4	11.5
$L_1^{(2)}$ ([1$\bar{1}\bar{1}$])	−6.20	0	−3.80	−3.83	11.4	11.5
$L_1^{(2)}$ ([1$\bar{1}$1] or [11$\bar{1}$])	−6.20	0	−3.80	−3.83	−11.4	−11.5
L_3 [111]	−2.86	±4.37	4.77	4.53	4.77±13.12	4.53±12.72
L_3 [1$\bar{1}\bar{1}$]	−2.86	±4.37	−1.59±8.75	−1.51±8.48	4.77±13.12	4.53±12.72
L_3 ([1$\bar{1}$1] or [11$\bar{1}$])	−2.86	±4.37	−1.59±8.75	−1.51±8.48	−4.77±13.12	−4.53±12.72
$L_{3'}$ [111]	−1.74	±4.87	6.25	6.10	6.25± 4.38	6.10± 4.03
$L_{3'}$ [1$\bar{1}\bar{1}$]	−1.74	±4.87	−2.08±2.92	−2.03±2.69	6.25± 4.38	6.10± 4.03
$L_{3'}$ ([1$\bar{1}$1] or [11$\bar{1}$])	−1.74	±4.87	−2.08±2.92	−2.03±2.69	−6.25± 4.38	−6.10± 4.03
$X_1^{(2)}$ ([100])	−1.80	6.38	±5.23	±5.23	±15.7	±15.7
$X_1^{(2)}$ ([010] or [001])	−1.80	−3.19	±5.23	±5.23	0	0
X_4 ([100])	0.58	5.26	±3.32	±3.32	±9.97	±9.97
X_4 ([010] or [100])	0.58	−2.63	±3.32	±3.32	0	0

tion to δV_{000} for all states just above the gap to be 15% less than that for all states just below the gap. Thus, from Table II of II: $\delta V_{000}^{\text{val}}=0.929$ Ry per unit dilation; $\delta V_{000}^{\text{cond.}}=0.897$ Ry per unit dilation. With these and the $\mathcal{H}$'s for a general strain we may as in I and II calculate the effect of any strain on the eigenvalues of the unstrained crystal Hamiltonian.

The various states at Γ, X, and L in the Brillouin zone have from one (e.g., $\Gamma_{2'}$) to as many as four (e.g., $L_{3'}$) independent deformation potential constants. We shall first consider the states at L. We have calculated the deformation potentials for the state $L_{3'}$ in the valence band and for the states L_1 and L_3 in the conduction band. (See Fig. 1.) The state L_1 is nondegenerate within a given [111] valley. There are, however, four equivalent [111] valleys. L_1 has two independent deformation potential constants, one corresponding to a hydrostatic strain, and one corresponding to a [111] uniaxial strain. The effect of a dilationless [111] strain on the L_1 valleys is to move the [111] valley a certain amount and to move the [11$\bar{1}$], [1$\bar{1}$1], and [1$\bar{1}\bar{1}$] each one third that amount in the opposite direction, the center of gravity of the four equivalent states remaining unchanged. The states $L_{3'}$ and L_3 would be twofold degenerate, were it not for spin-orbit splitting. If one neglects spin-orbit splitting, each of these (L_3 and $L_{3'}$) has four independent deformation-potential constants. In addition to the two which L_1 boasts, there are two independent strains which split the degeneracy, a uniaxial [100] strain and a yz shear strain. These strains destroy the threefold rotation axes which caused the degeneracies. A [111] strain does not destroy the threefold rotation axis in the [111] direction, but does destroy those axes along the [1$\bar{1}\bar{1}$], [1$\bar{1}$1], and [11$\bar{1}$] directions, thereby splitting the L_3 and $L_{3'}$ degeneracies in those valleys. However, this splitting is not independent of that caused by a yz shear since a dilationless [111] strain tensor may be written

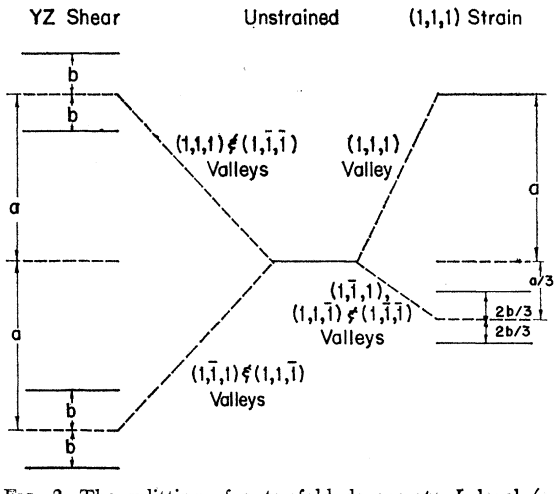

FIG. 2. The splitting of a twofold degenerate L level (e.g., L_3 or $L_{3'}$) under a [111] strain or a yz shear. a and b are two independent deformation potential constants.

$$\mathcal{E}[111]=\tfrac{1}{3}\begin{vmatrix}0&1&1\\1&0&1\\1&1&0\end{vmatrix}=\tfrac{1}{3}\begin{vmatrix}0&1&1\\1&0&-1\\1-1&0\end{vmatrix}+\tfrac{2}{3}\begin{vmatrix}0&0&0\\0&0&1\\0&1&0\end{vmatrix}$$
$$=-\mathcal{E}[1\bar{1}\bar{1}]+\tfrac{2}{3}\mathcal{E}(yz)\,. \quad (4)$$

Thus, since $\mathcal{E}[111]$ causes no splitting within a [111] valley, we see that $\mathcal{E}[111]$ splits L_3 and $L_{3'}$ in the $[1\bar{1}\bar{1}]$ valley $\frac{2}{3}$ as much as a (yz) shear. A yz shear strain shifts both the [111] and $[1\bar{1}\bar{1}]$ valleys as much as a [111] strain shifts a [111] valley, while under a yz shear strain, the $[1\bar{1}1]$ and $[11\bar{1}]$ valleys move equally in the opposite direction. Furthermore, the intervalley degeneracies are split identically in the four valleys (see Fig. 2). The effect of a [111] strain is also shown in Fig. 2. On the other hand, a [100] strain cannot distinguish between L valleys and only splits the intravalley degeneracies. The total strain plus spin-orbit splitting is given by[18]

$$\Delta=(\Delta_{so}^2+\Delta_{strain}^2)^{1/2}, \tag{5}$$

where Δ_{so} is the spin-orbit splitting in the absence of strain and vice versa. Thus when $\Delta_{so}\gg\Delta_{strain}$, $\Delta\approx\Delta_{so}+\Delta_{strain}^2/2\Delta_{so}$ and the strain splitting becomes a second-order effect. Similarly, the spin-orbit splitting becomes a second-order effect when $\Delta_{strain}\gg\Delta_{so}$. The shear strain intravalley deformation potential is rather large for L_3 (see Table I) and $\Delta_{strain}=0.05$ eV should be attainable with large strains. According to Phillips and Liu[19], in Ge $\Delta_{so}^{L_{3'}}=0.18$ eV, while because of interference effects $\Delta_{so}^{L_3}=0.01$ eV. Presumably the corresponding splittings in Si are an order of magnitude smaller. Thus both limits $\Delta_{so}\gg\Delta_{strain}$ and $\Delta_{strain}\gg\Delta_{so}$ are of practical interest.

All X levels in a diamond-structure crystal are forced to be twofold degenerate by the existence of the glide symmetry operations. Specifically, an x direction X level is split if both the xy and xz glide planes are destroyed. These may be destroyed by a yz shear. While a yz shear splits the [100] X level, it does not split the [010] or [001] levels and does not shift the X valleys with respect to one another. A [111] strain, being a sum of $\frac{1}{3}$ of each of the three shears, splits all levels $\frac{1}{3}$ as much as a yz shear splits a [100] level. A [100] strain moves the [100] valley up and moves both the [010] and [001] valleys down by half as much without splitting the intravalley degeneracies.

The $\Gamma_{2'}$ level, having the full cubic symmetry and being only spin degenerate is affected only by the hydrostatic component of an applied strain. Similarly (since for all but the largest strains in Si, $\Delta_{so}\gg\Delta_{strain}$), the $j=\frac{1}{2}$ spin-orbit split $\Gamma_{25'}$ and Γ_{15} levels are described by a single hydrostatic deformation potential. The $j=\frac{3}{2}\Gamma_{25'}$ and Γ_{15} levels are fourfold degenerate. These may be split into $|m_j|=\frac{3}{2}$ and $|m_j|=\frac{1}{2}$ twofold degenerate levels by either a [100] or [111] strain. Each of these strains gives an independent deformation potential constant. A more thorough discussion of the $\Gamma_{25'}$ deformation potentials is given in I.

III. RESULTS AND CONCLUSIONS

The calculations were performed using the complete wave functions of Kleinman and Phillips[20] which are expanded in plane waves. In the hand calculations of I and II, many terms involving small coefficients of the plane waves were neglected. Thus, the present $\Gamma_{25'}$ hydrostatic deformation potential is about 10% larger than the hand calculation. On the other hand, the two uniaxial $\Gamma_{25'}$ deformation potentials converged in the previous calculation to within a fraction of a percent. There is much cancellation between positive and negative terms; this takes place among $\mathcal{K}_{KE}'$, $\mathcal{K}_{PE}'$, and $\mathcal{K}_R'$ and causes the rapid convergence in the uniaxial strain case. In the hydrostatic strain case, most of the cancellation occurs between δV_{000} on the one hand and $\mathcal{K}_{KE}'+\mathcal{K}_{PE}'+\mathcal{K}_R'$ on the other; the poorer convergence is due to the smallness of the cancellation among $\mathcal{K}_{KE}'$, $\mathcal{K}_{PE}'$, and $\mathcal{K}_R'$. In Table I we list the deformation potentials in units of eV per unit strain for all the levels discussed in the previous section under hydrostatic, [100], [111], and [011] strains. The results for the latter two strains are listed for the experimental value[15] of the bond bending parameter ($\zeta=0.7$) as well as for the value that gives the experimental ratio of the two $\Gamma_{25'}$ uniaxial strain deformation potential constants ($\zeta=0.81$). Because of the calculational errors in I, we list in Table II D_u and $D_{u'}$ where $|\frac{4}{3}D_u|$ is the splitting of $\Gamma_{25'}$ per unit [100] uniaxial strain and $|\frac{4}{3}D_{u'}|$ plays the same role for [111] strain. The comparison with the experimental values[1] is worsened, but considering the large cancellation among the various terms in the Hamiltonian[21] and the uncertainties in the unperturbed wave functions, the agreement should be considered satisfactory. We also list the experimental values for Ge since this is the only case of a degeneracy splitting which has been measured in both materials.

TABLE II. Comparison of experimental values of D_u and D_u' (in eV) in[a] Si and[b] Ge with two calculated values for Si. The choice of $\zeta=0.81$ for one of these is to make the calculated $D_u'D_u$ agree with the experimental Si value; $\zeta=0.7$ is the value in Ge obtained from x-ray scattering.[c]

	Si exp.	Ge exp.	$\zeta=0.7$	$\zeta=0.81$
D_u	2.04	3.15	3.74	3.74
$D_{u'}$	2.68	6.06	4.19	4.92
$D_{u'}/D_u$	1.31	1.92	1.12	1.31

[a] Ref. 1.
[b] J. J. Hall, Phys. Rev. **128**, 68 (1962).
[c] Ref. 15.

[18] Consider the [111] valley and a shear strain (yz) or a uniaxial strain (xx). The degenerate transverse p eigenfunctions without the spin-orbit or strain perturbations may be chosen to have $(x-y)$ and $(x+y-2z)$ symmetry. These are obviously diagonal under perturbations of (yz) or (xx) symmetry while they are off diagonal under the spin-orbit perturbation. Equation (5) follows directly from diagonalizing the perturbation matrix.

[19] J. C. Phillips and L. Liu, Phys. Rev. Letters **8**, 94 (1962); and L. Liu, Phys. Rev. **126**, 1317 (1962).

[20] L. Kleinman and J. C. Phillips, Phys. Rev. **118**, 1153 (1960).

[21] The reader is referred to I and II to obtain an idea of the order of magnitude of the various contributions to the deformation potentials.

TABLE III . Calculated and experimental values of Ξ_u in the notation of Herring and Vogt.[a] This is $\frac{2}{3}$ the deformation potential listed in Table I for the shift of [100] valley under a [100] strain and is equal to that listed in Table I for the shift of a [111] valley under a [111] strain. The experimental value in Si is determined for the valley which is near but not exactly at the symmetry point X.

	Experimental	Theoretical
X_1	11,[b] 8.3[d] (Si)	9.57 (Si)
L_1	19 (Ge)[c]	11.4 (Si)

[a] Ref. 11.
[b] Ref. 4.
[c] Ref. 5.
[d] J. E. Aubrey, W. Gubler, T. Henningsen, and S. H. Koenig, Phys. Rev. 130, 1667 (1963).

In Table III we compare experimental and theoretical values of Ξ_u (notation of Herring and Vogt[11]) which describes the shift between a conduction band valley and its equivalent valleys when a uniaxial strain is applied along its major axis. In Si the valleys lie along [100] near but not at the symmetry point X so that the good agreement between theory and experiment may be somewhat fortuitous. Judging from the experimental differences between Ge and Si for the splitting of $\Gamma_{25'}$, (Table II), we should expect only order of magnitude agreement between the theoretical value of Ξ_u for L_1 in Si and its experimental value in Ge. The agreement is therefore quite satisfactory.

In Table IV we compare calculated and experimental values of various gap dependencies in units of eV per 10^6 atm. Unfortunately, most of the data is for Ge, however, the gap dependencies as a function of *pressure* are known to be similar for all the diamond and zincblende crystals.[9] The percentage error between the experimental $\Delta_1-\Gamma_{25'}$ and the theoretical $X_1-\Gamma_{25'}$ gap dependencies is quite large but this is because of the extremely small value of the gap dependence. Since the gap dependence is small because of extremely good cancellation between much larger absolute shifts of X_1 and $\Gamma_{25'}$ and not because the individual shifts are small, this large percentage error is to be expected. The overall agreement is seen to be quite good.

TABLE IV. Comparison of experimental and calculated gap dependencies in units of eV per 10^6-atm hydrostatic pressure.

	Experimental	Calculated (Si)
L_1–$\Gamma_{25'}$	5.0 Ge[a]	4.27
$\Gamma_{2'}$–$\Gamma_{25'}$	12.0 Ge[a]	8.93
Δ_1–$\Gamma_{25'}$	−1.5 Si[a,b]	−0.30[c]
L_1–$L_{3'}$	7.5 Ge[d]	4.62

[a] Ref. 6.
[b] Ref. 7.
[c] The calculated gap is X_1–$\Gamma_{25'}$.
[d] R. Zallen, W. Paul, and J. Tauc, Bull. Am. Phys. Soc. 7, 185 (1962).

Note added in proof. R. Zallen and W. Paul (private communication), measuring the reflectivity of Si under hydrostatic pressure, have obtained the following gaps:

$$E_\Gamma = 3.38 + 5.2P,$$
$$E_x = 4.4 + 2.9P,$$

where E is in eV and P in 10^6 atm. The latter gap, which they identify with an X_4-X_1 transition, has a pressure coefficient in good agreement with our value of 2.4. The first gap, which they identify with a $\Gamma_{25'}-\Gamma_{15}$ transition, has a pressure coefficient in sharp disagreement with our value of 1.4. We feel that this throws considerable doubt on the identification of this level. One is tempted to identify the 3.38-eV reflection peak with the $L_1-L_{3'}$ transition for which we have a calculated pressure coefficient of 4.5 eV/10^6 atm.

The largest errors in our calculated deformation potentials are due to errors in the undeformed crystal wave functions and to the approximations made in calculating the strain dependence of the self-consistent valence electron potential (see I and II). Crystal potentials can be obtained which yield energy bands in excellent agreement with experiment; presumably the wave functions will be just as good. These should be available in the immediate future.[22] A better calculation of the strain dependence of the self-consistent potential would require essentially a complete self-consistent band calculation for the strained crystal. We think that with these improvements, it should be possible to calculate deformation potentials accurate to within 10%.

[22] F. Quelle (private communication) and F. Herman (private communication).